

# Bis(amidophenolato)phosphonium: Si–H Hydride Abstraction and Phosphorus-Ligand Cooperative Activation of C–C Multiple Bonds

Daniel Roth,<sup>[a]</sup> Thaddäus Thorwart,<sup>[a]</sup> Clara Douglas,<sup>[a, b]</sup> and Lutz Greb\*<sup>[a, b]</sup>

**Abstract:** The first bis(amidophenolato)phosphonium salts are prepared and fully characterized. The perfluorinated derivative represents the strongest monocationic phosphorus Lewis acid on the fluoride and hydride ion affinity scale isolable to date. This affinity enables new reactions, such as hydride abstraction from Et<sub>3</sub>SiH, the first phosphoalkoxylation of an

alkyne or a phosphorus catalyzed intramolecular hydroarylation. All properties and reactions are scrutinized by theory and experiment. Substantial  $\sigma$ - and  $\pi$ -acidity provides the required affinity for substrate activation, while phosphorus-ligand cooperativity substantially enriches the reactivity portfolio of phosphonium ions.

## Introduction

Continuous interest has been awarded to the development of Lewis acidic electrophilic phosphorus cations (EPC) in recent years. Spearheaded by the preparation of the fluorophosphonium ion  $\text{FP}(\text{C}_6\text{F}_5)_3^+$  (Figure 1a), related electrophilic compounds have unlocked new possibilities in Lewis acid catalysis.<sup>[1]</sup> In this vein, we introduced a class of phosphonium ions, where structural constraint through rigid catecholato ligands empowered extreme Lewis acidity (Figure 1c).<sup>[2]</sup> This strategy successfully provided the first neutral silicon and germanium Lewis superacids.<sup>[3]</sup> Herein we report the class of bis(amidophenolato)phosphonium ions. The ligand variation imparts an effective means to alter the electronics and sterics at phosphorus while simultaneously controlling the tendency for phosphorus ligand-cooperative (PLC) bond activation reactions.<sup>[4]</sup> Previous examples for amidophenolato substituted phosphorus compounds comprise organo-<sup>[5]</sup> and metallaphosphoranes<sup>[6]</sup> (Figure 1b), as well as investigations on the tris(amidophenolato)phosphate scaffold.<sup>[7]</sup> Very recently, Dobrovetsky and Alcarazo described an exciting tethered ONNO bis(amidophenolato)ligand to create structurally constrained phosphorus species with unique reactivity (Figure 1b).<sup>[8]</sup>

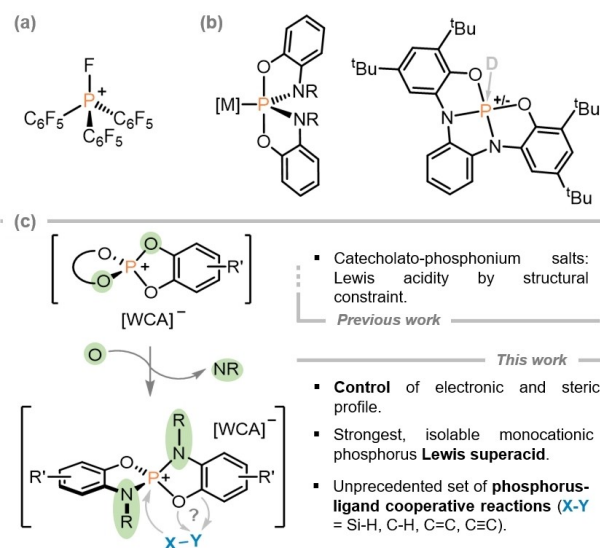


**Figure 1.** a) Seminal fluorophosphonium Lewis acid. b) Metallaphosphoranes and geometrically constrained P species of the N,O-ligand. c) Comparison of this work to previous catecholato-phosphonium Lewis acids.

However, free tetracoordinate phosphonium ions of the ON-ligand type and their reactivity have remained elusive thus far. It turns out that the combination of highly Lewis acidic phosphonium with a fairly nucleophilic ligand scaffold empowers several unique PLC reactivity modes.

## Results and Discussion

The aminophenoles **1a** and **1b** were prepared by literature-known procedures and are accessible within one or two high-yielding steps at a multigram scale (Figure 2).<sup>[7,9]</sup> Fully fluorinated **1c** was recently introduced as a ligand for the preparation of a highly Lewis acidic silane and is easily prepared via a three-step procedure starting from hexafluorobenzene.<sup>[10]</sup>

[a] D. Roth, T. Thorwart, C. Douglas, Prof. L. Greb  
Anorganisch-Chemisches Institut  
Ruprecht-Karls-Universität Heidelberg  
Im Neuenheimer Feld 270, 69120 Heidelberg (Germany)  
E-mail: lutz.greb@fu-berlin.de

[b] C. Douglas, Prof. L. Greb  
Department of Chemistry and Biochemistry - Inorganic Chemistry  
Freie Universität Berlin  
Fabeckstr. 34/36, 14195 Berlin (Germany)

Supporting information for this article is available on the WWW under <https://doi.org/10.1002/chem.202203024>

© 2022 The Authors. Chemistry - A European Journal published by Wiley-VCH GmbH. This is an open access article under the terms of the Creative Commons Attribution Non-Commercial License, which permits use, distribution and reproduction in any medium, provided the original work is properly cited and is not used for commercial purposes.

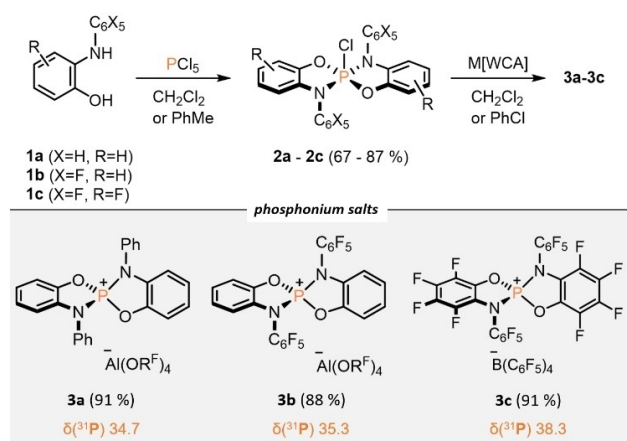


**Figure 2.** Synthesis of chlorophosphoranates **2a–2c** and transformation into the bis(amidophenolato)phosphonium salts **3a–3c**. ( $R^F = \text{C}(\text{CF}_3)_3$ ).

Reacting the aminophenols with  $\text{PCl}_5$  proceeded with the liberation of  $\text{HCl}$  and yielded the respective bis(amidophenolato)chlorophosphoranates **2a–c** in good to excellent yields after workup.<sup>[11]</sup>

While the reaction with **1c** occurred readily at room temperature, more forcing conditions were required with **1a/b**. The respective phosphonium salts were obtained by salt metathesis of **2a** and **2b** with  $\text{Li}[\text{Al}(\text{OR}^F)_4]$  ( $R^F = \text{C}(\text{CF}_3)_3$ ), furnishing **3a** and **3b** in excellent yields. No reaction, however, was observed with **2c**. Attempts to generate the cation with the more potent  $\text{Et}_3\text{Si}[\text{BArF}_{20}]$  in benzene or toluene were unsuccessful, hinting at a substantial chloride ion affinity of **3c**. Switching the solvent to less coordinating chlorobenzene enabled the chloride abstraction, generating the perfluorinated phosphonium salt **3c** in excellent yield. With an increasing degree of fluorination, an increased deshielding of the central phosphorus atom is observed, leading to  $^{31}\text{P}$  NMR signals ranging from 34.7 ppm for **3a**, 35.3 ppm for **3b** to 38.3 ppm for perfluorinated **3c**. Unlike **3a** and **3b**, **3c** is only poorly soluble

**Table 1.** Computed fluoride and hydride ion affinities at the DLPNO-CCSD(T)/def2-TZVPP// $\omega$ B97X-D3(BJ)/def2-TZVPP (COSMO-RS)<sup>[13]</sup> level of theory. Entries 1–3, 7–8 obtained from reference.<sup>[2]</sup> Gutmann-Beckett  $^{31}\text{P}$  NMR shifts vs. free  $\text{OPeEt}_3$  in  $\text{CD}_2\text{Cl}_2$ .

	Compound	FIA [ $\text{kJmol}^{-1}$ ]	HIA [ $\text{kJmol}^{-1}$ ]	GB-shift
1	$[\text{P}(\text{cat}^{\text{H}})_2]^+$	776 (303)	825 (486)	55.6
2	$[\text{P}(\text{cat}^{\text{Bu}})_2]^+$	739 (292)	787 (474)	53.3
3	$[\text{P}(\text{cat}^{\text{Bu}})(\text{cat}^{\text{Cl}})]^+$	792 (330)	845 (517)	58.8
4	$[\text{P}(\text{aph}^{\text{Ph}})_2]^+$ <b>3a</b>	687 (245)	743 (430)	45.5
5	$[\text{P}(\text{aph}^{\text{C}_6\text{F}_5})_2]^+$ <b>3b</b>	750 (296)	808 (485)	50.6
6	$[\text{P}^{\text{F}}(\text{aph}^{\text{C}_6\text{F}_5})_2]^+$ <b>3c</b>	<b>825 (352)</b>	<b>890 (550)</b>	58.4
7	$[(\text{C}_6\text{F}_5)_3\text{PF}]^+$	717 (248)	799 (461)	40.4
8	$\text{B}(\text{C}_6\text{F}_5)_3$	445 (249)	471 (401)	30.6

in dichloromethane, but good solubility is observed in *o*-difluorobenzene. The salts can be prepared up to a multigram scale and stored over months at room temperature as solids under an inert atmosphere. In solution, slow decomposition via fluoride abstraction from the  $\text{BArF}_{20}$  counteranion was observed over weeks.

Single crystals suitable for X-ray diffraction were obtained for all phosphonium salts by either vapor diffusion of pentane into or directly cooling concentrated solutions in dichloromethane (Figure 3). The solid-state structures show the monomeric nature and distorted tetrahedral coordination geometry around the central phosphorus. Bond lengths and angles of all structures are similar and in the expected range of P–N and P–O bonds (see table S1). The only significant difference is the apparent stacking of the  $-\text{C}_6\text{F}_5$  groups of **3b/3c** compared to the phenyl groups of **3a** (angles of the aromatic planes relative to each other were measured at 5.4 and 16.3° for **3b** and **3c** vs. 24.6° for **3a**). This is attributed to the increase in dispersion interaction introduced by the heavier fluorine atoms, favoring the coplanar orientation.<sup>[12]</sup>

For the assessment of *global* Lewis acidity, fluoride (FIA) and hydride (HIA) ion affinities were computed in the gas phase and with a solvent model (Table 1). Fluorination of the amidophenolate backbone has a stronger impact over fluorination of the *N*-

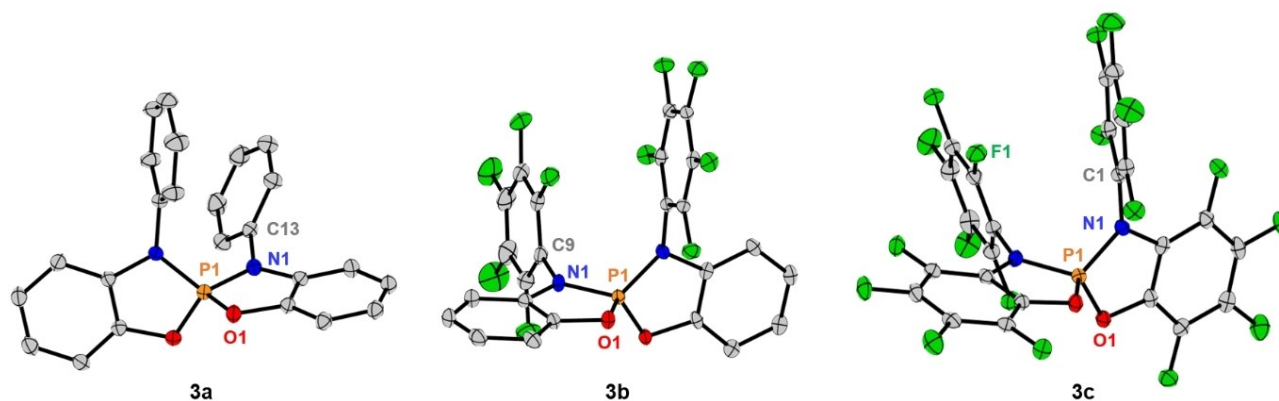


**Figure 3.** SCXRD derived molecular structures of phosphonium ions **3a**, **3b** and **3c**. Ellipsoids are displayed at 50% probability, hydrogens and counteranions were omitted for clarity. Selected bond lengths [ $\text{\AA}$ ] and angles [deg]: **3a**: P1–N1 = 1.6266(13), P1–O1 = 1.5741(12), N1–C13 = 1.450(2), O1–P1–N1 = 97.90(6); **3b**: P1–N1 = 1.630(2), P1–O1 = 1.572(2), N1–C9 = 1.425(4), O1–P1–N1 = 97.42(12); **3c**: P1–N1 = 1.6304(17), P1–O1 = 1.5683(15), N1–C1 = 1.438(3), O1–P1–N1 = 97.93(8).

substituted phenyl ring. The obtained values suggest that **3c** constitutes the most potent isolable monocationic phosphonium ion, surpassing all previously isolable catecholato-phosphonium ions by over 30 kJ mol<sup>-1</sup>.

To assess the *effective* Lewis acidity of these phosphonium ions, triethylphosphine oxide (TEPO) was added in dichloromethane according to the Gutmann-Beckett (GB) method.<sup>[14]</sup> The emergence of two new pairs of doublets in the <sup>31</sup>P{<sup>1</sup>H} NMR spectra with matching coupling constants indicated adduct formation. The relative shifts of the <sup>31</sup>P NMR signals of the bound TEPO followed the expected order and demonstrated substantial Lewis acidity also on the Gutmann-Beckett scale (Table 1). While **3b** seems to be a stronger Lewis acid on the anion affinity scale compared to [P(cat<sup>bu</sup>)<sub>2</sub>]<sup>+</sup>, the order is reversed on the GB scale, likely due to steric reasons.

The reactivity of these compounds with silanes was probed and compared with the catecholato-phosphonium ions (Figure 4). Adding Et<sub>3</sub>SiH to **3a** led to no reaction, while **3b** and **3c** showed immediate reaction upon mixture.

The reaction with **3b** did not proceed cleanly, whereas selective hydride abstraction was observed when **3c** and Et<sub>3</sub>SiH were mixed in CD<sub>2</sub>Cl<sub>2</sub>, resulting in the formation of phosphorane **4** (Figure 4a) with a signal in the <sup>31</sup>P NMR at -49.6 ppm and a characteristically large coupling constant (<sup>1</sup>J<sub>PH</sub> = 928.7 Hz) indicative of a P(V)-H species (Figure 4b). X-ray diffraction analysis of crystals obtained by gas phase diffusion of pentane into the reaction solution confirmed the molecular structure (Figure 4c). In line with this observation, the solvent-corrected HIA of **3c** in CH<sub>2</sub>Cl<sub>2</sub> was computed higher than that of Et<sub>3</sub>Si<sup>+</sup> by 25 kJ mol<sup>-1</sup>. The formed triethylsilylium cation is unstable in dichloromethane and decomposes to several species, including Et<sub>3</sub>SiCl/F by halide abstraction from the solvent and counteranion. To the best of our knowledge, this is the first unequivocal

evidence of hydride abstraction from a silane by a phosphonium ion - a commonly proposed step in phosphonium ion-mediated reduction catalysis.<sup>[11]</sup> Interestingly, analog reactions of the bis(catecholato) phosphonium ion P(cat<sup>h</sup>)<sub>2</sub><sup>+</sup> with silanes did not result in mere hydride abstraction. Instead, the addition of the Si-H moiety along the P-O bond in PLC-fashion yielded phosphonium cation **5** (δ <sup>31</sup>P = 36.0 ppm, <sup>1</sup>J<sub>PH</sub> = 946 Hz, Figure 4d). Umpolung of the formerly hydridic silane hydrogen to an acidic proton allowed easy deprotonation by a relatively weak base such as triphenylphosphine. The resulting phosphite could be isolated as a colorless oil, and structural evidence was obtained by complexation of the phosphite with (PhCN)<sub>2</sub>PdCl<sub>2</sub>, yielding the dinuclear palladium complex [Pd<sub>2</sub>Cl<sub>4</sub>]-**6**<sub>2</sub>, as confirmed by scXRD (Figure 4e). Computational studies confirmed a favorable silyl group transfer from the intermediary phosphonium-silane σ-adduct (see Supporting Information).

The addition of 3-hexyne to a solution of **3b** results in the selective and immediate reaction to a single product with a singlet in the <sup>31</sup>P NMR at 24.6 ppm. Integration of <sup>1</sup>H NMR signals indicated a 1:1 adduct of phosphonium ion and alkyne. The combined analytical features were consistent with product **8**, containing a phosphine oxide connected to an indolium fragment (Figure 5a).

The reaction of **3c** with tolane (and other aromatic alkynes) gave products equivalent to **8** (Figure 5b). Slow evaporation of solvent from a dichloromethane solution provided single crystals for X-ray diffraction, giving structural evidence for the connectivity of **9** (Figure 5c). DFT calculations at the DSD-BLYP-D3(BJ)/def2-QZVPP+SMD(CH<sub>2</sub>Cl<sub>2</sub>)/r<sup>2</sup>-SCAN-3c level of theory showed that the reaction likely proceeded by initial cooperative addition of the alkyne via dearomatization of the amidophenolate ligand to give intermediate **7a** (Figure 5a).<sup>[15]</sup> Such a reactivity mode had been observed for antimony amidophenolates in reaction with dioxygen but is unknown for phosphorus.<sup>[16]</sup> Subsequent rearrangement to **7b** and a final 1,2-shift of the phosphorus yields the more stable isomer **8**, containing an iminium ion instead of a carbocation. Alternative additions along the P-O or P-N bonds are computed to be kinetically prohibited (for details, see the Supporting Information).

Interestingly, the reaction of **3c** with the terminal alkyne phenylacetylene yielded the regioisomeric and neutral product **11** with the P-part placed at the α-position of the formed indole (Figure 5b). Apparently, deprotonation from an intermediate of type **7b** is more rapid than the 1,2-shift leading to products **8** and **9**, where such protons are missing. These observations further corroborate the mechanism depicted in Figure 5a.

Yet another outcome was observed during the reaction of 3-hexyne with **3c** (Figure 5b). <sup>1</sup>H NMR integration of signals again indicated a 1:1 addition product, while multidimensional NMR-spectroscopic data confirmed the addition proceeding across the P-O bond to give **12**. This pattern is further supported by fitting computed <sup>31</sup>P NMR shifts and mechanistic elucidation (see section 6d in Supporting Information).<sup>[17]</sup> Interestingly, the aryl-attack leading to an intermediate of type **7a** is disfavored with the electron-deficient **3c**, but a P-O

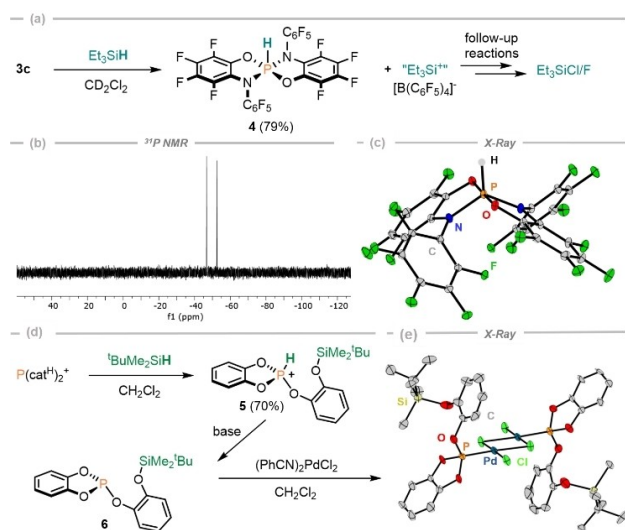


**Figure 4.** (a) Reaction of **3c** with Et<sub>3</sub>SiH, (b) <sup>31</sup>P NMR spectrum and (c) solid-state structure of the reaction product **4**. (d) Reaction of P(cat<sup>h</sup>)<sub>2</sub><sup>+</sup> with tBuMe<sub>2</sub>SiH (BARF<sub>20</sub><sup>-</sup> counterion omitted for clarity) and (e) solid-state structure of the palladium-complex of phosphite **6**. Conversion rates to the products were estimated from <sup>31</sup>P NMR.

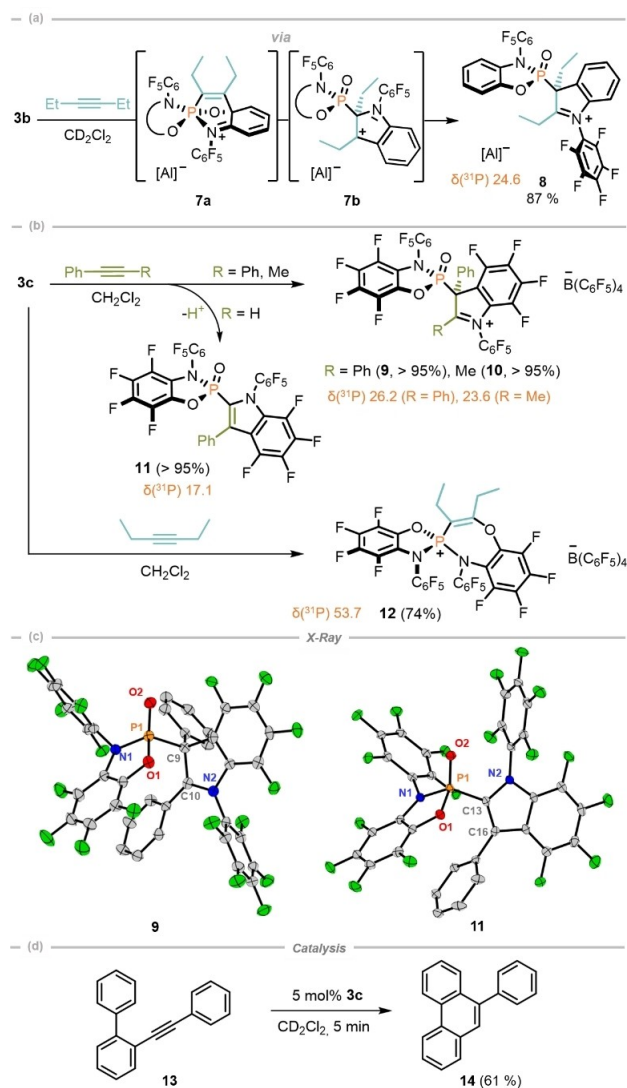


**Figure 5.** (a) Reaction of **3b** with 3-hexyne including calculated intermediates, isolated yield is given, (b) reaction of **3c** with different aromatic alkynes, conversion rates to the products were estimated from  $^{31}\text{P}$  NMR, (c) solid-state structures of **9** and **11**, ellipsoids set at 50% probability, hydrogen atoms and the counteranion of **9** were omitted for clarity, selected bond lengths [Å]: **9**: P1–O2 = 1.4452(15), P1–O1 = 1.6180(14), P1–N1 = 1.6899(17), C9–C10 = 1.521(3), C10–N2 = 1.327(2); **11**: P1–O2 = 1.4601(19), P1–O1 = 1.6121(18), P1–N1 = 1.695(2), C13–C16 = 1.368(3), C13–N2 = 1.409(3), (d) exemplary catalysis, isolated yield is given.

cleavage now becomes the preferred pathway. To our knowledge, this reaction corresponds to the first report of a phosphoalkoxylation of a C–C multiple bond. Of note here is a reaction of an oxaphosphete cation with acetonitrile to form the six-membered phosphorus heterocycle found by Dielmann.<sup>[18]</sup>

This set of transformations showcased the pronounced ability of bis(amidophenolato)phosphonium ions to act as  $\pi$ -acids. Hence, we were interested if catalytic cycles could be initiated upon offering a substrate that contains a nucleophilic group able to compete with the intramolecular PLC mode described above. Indeed, catalytic intramolecular hydroarylation

of alkyne substrate **13** to 9-phenylphenanthrene **14**, yielded the 6-*endo* cyclization product in moderate isolated yields (Figure 5d).

**3c** also reacts smoothly with heteroarenes to directly form the P-functionalized heteroarenes (Figure 6a). For instance, the reactions with thiophene and 2-bromothiophene proceed quickly, and the deprotonated product is formed almost immediately upon mixing. A second equivalent of arene served as a base here to deprotonate the highly Brønsted acidic intermediate. The product of the thiophene reaction was confirmed by scXRD (Figure 6b).

Compared to the analogous reaction with the catecholato-phosphonium ions, this reaction proceeds faster, and the corresponding intermediate addition product containing the phenolic OH-moiety was not detected.<sup>[2]</sup> Finally, rapid reactions were also observed with alkenes. NMR spectroscopic analysis of a reaction mixture of **3b** with 2-norbornene indicated **17** as the major and regioisomeric **18** as a minor product (Figure 6c). Isolation was not attempted, but the identity of **17** was confirmed by scXRD (Figure 6d). Interestingly, **17** results from an initially formed nonclassical 2-norbornyl cation.<sup>[19]</sup> A spontaneous reaction of **3c** was also observed with less activated alkenes such as 1-methylcyclohexene, but the formation of multiple isomers prevented the identification of the exact product connectivity thus far.

## Conclusion

In summary, this work describes the first isolation of bis(amidophenolato)phosphonium ions and significantly extends the range of reactivity modes of phosphorus cations. Compared to the bis(catecholato)phosphonium ions, even higher Lewis acidities are reached, and complementary reactivity is

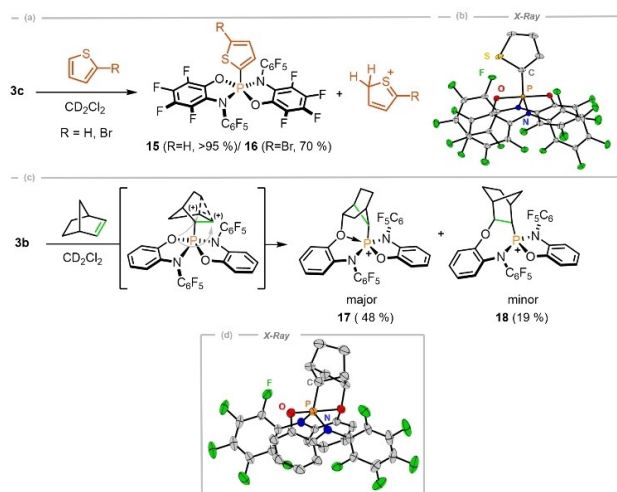


**Figure 6.** (a) Reaction of **3c** with different thiophene derivatives. (b) Solid-state structures of **15** and **17** (ellipsoids set at 50 and 30% probability, respectively), hydrogen atoms and the counteranion of **17** were omitted for clarity. (c) Reaction of **3b** with 2-norbornene (products not isolated). Conversion rates to the products were estimated from  $^{31}\text{P}$  NMR.



noted. Based on the degree of fluorination of the amidophenolato ligands, varying reactivity toward Si–H and multiple C–C bond substrates is identified. The rapid alkyne and alkene activations indicate multiple entry points for follow-chemistry and promise novel opportunities for  $\pi$ - and  $\sigma$ -catalysis with this class of Lewis superacids.

## Experimental Section

For experimental details, see the Supporting Information.

Deposition Numbers 2206700, 2206701, 2206702, 2206703, 2206704, 2206705, 2206706, 2206707, 2206708, 2206709, and 2206710 contain the supplementary crystallographic data for this paper. These data are provided free of charge by the joint Cambridge Crystallographic Data Centre and Fachinformationszentrum Karlsruhe Access Structures service.

## Acknowledgements

The authors acknowledge support by the state of Baden-Württemberg through bwHPC and the German Research Foundation (DFG) through grant no INST 40/575-1 FUGG (JUSTUS 2 cluster). D.R. is grateful to the FCI for a Kekulé fellowship. M. Schorpp is acknowledged for help with the solution of scXRD structures. Open Access funding enabled and organized by Projekt DEAL.

## Conflict of Interest

The authors declare no conflict of interest.

## Data Availability Statement

The data that support the findings of this study are available in the supplementary material of this article.

**Keywords:** amidophenolate · element-ligand cooperativity · Lewis superacid ·  $\pi$ -activation · phosphonium

- [1] a) C. B. Caputo, L. J. Hounjet, R. Dobrovetsky, D. W. Stephan, *Science* **2013**, *341*, 1374–1377; b) J. Bayne, D. Stephan, *Chem. Soc. Rev.* **2016**, *45*, 765–774; c) D. W. Stephan, *Angew. Chem. Int. Ed.* **2017**, *56*, 5984–5992; *Angew. Chem.* **2017**, *129*, 6078–6086.
- [2] D. Roth, J. Stirn, D. W. Stephan, L. Greb, *J. Am. Chem. Soc.* **2021**, *143*, 15845–15851.
- [3] a) R. Maskey, M. Schädler, C. Legler, L. Greb, *Angew. Chem. Int. Ed.* **2018**, *57*, 1717–1720; *Angew. Chem.* **2018**, *130*, 1733–1736; b) D. Hartmann, M. Schädler, L. Greb, *Chem. Sci.* **2019**, *10*, 7379–7388; c) D. Roth, H. Wadepohl, L. Greb, *Angew. Chem. Int. Ed.* **2020**, *59*, 20930–20934; *Angew. Chem.* **2020**, *132*, 21116–21120.
- [4] a) Y.-C. Lin, E. Hatzakis, S. M. McCarthy, K. D. Reichl, T.-Y. Lai, H. P. Yennawar, A. T. Radosevich, *J. Am. Chem. Soc.* **2017**, *139*, 6008–6016; b) L. Greb, F. Ebner, Y. Ginzburg, L. M. Sigmund, *Eur. J. Inorg. Chem.* **2020**, *2020*, 3030–3047; c) J. M. Lipshultz, G. Li, A. T. Radosevich, *J. Am. Chem. Soc.* **2021**, *143*, 1699–1721; d) C.-X. Guo, K. Schwedtman, J. Fidelius, F. Hennesdorf, A. Dickschat, A. Bauzá, A. Frontera, J. J. Weigand, *Chem. Eur. J.* **2021**, *27*, 13709–13714.
- [5] a) H. R. Allcock, R. L. Kugel, *Chemical Communications (London)* **1968**, *24*, 1606–1607; b) T. Koizumi, Y. Watanabe, Y. Yoshida, E. Yoshii, *Tetrahedron Lett.* **1974**, *15*, 1075–1078; c) C. Malavaud, J. Barrans, *Tetrahedron Lett.* **1975**, *16*, 3077–3080; d) C. D. Reddy, S. S. Reddy, M. S. R. Naidu, *Synthesis* **1980**, *1980*, 1004–1005; e) J. Hernández-Díaz, R. Contreras, B. Wrackmeyer, *Heteroat. Chem.* **2000**, *11*, 11–15; f) S. A. Terent'eva, I. L. Nikolaeva, A. R. Burilov, D. I. Kharitonov, E. V. Popova, M. A. Pudovik, I. A. Litvinov, A. T. Gubaidullin, A. I. Kononov, *Russ. J. Gen. Chem.* **2001**, *71*, 389–395; g) S. A. Terent'eva, M. A. Pudovik, A. T. Gubaidullin, I. A. Litvinov, A. N. Pudovik, *Russ. J. Gen. Chem.* **2001**, *71*, 330–336; h) H. R. Allcock, R. L. Kugel, *J. Am. Chem. Soc.* **2002**, *91*, 5452–5456; i) H. R. Allcock, R. L. Kugel, G. Y. Moore, *Inorg. Chem.* **2002**, *41*, 2831–2837; j) D. Krasowska, J. Chrzanowski, P. Kielbasiński, J. Drabowicz, *Molecules* **2016**, *21*; k) N. J. O'Brien, Y. Koda, H. Maeda, N. Kano, *Polyhedron* **2020**, *192*.
- [6] a) K. Kubo, H. Nakazawa, K. Kawamura, T. Mizuta, K. Miyoshi, *J. Am. Chem. Soc.* **1998**, *120*, 6715–6721; b) H. Nakazawa, K. Kawamura, K. Kubo, K. Miyoshi, *Organometallics* **1999**, *18*, 2961–2969; c) H. Nakazawa, K. Kubo, K. Miyoshi, *Bull. Chem. Soc. Jpn.* **2001**, *74*, 2255–2267; d) B. J. Jelier, C. D. Montgomery, F. G. L. Parlane, *Inorg. Chim. Acta* **2014**, *413*, 121–127.
- [7] C. Zhan, Z. Han, B. O. Patrick, D. P. Gates, *Dalton Trans.* **2018**, *47*, 12118–12129.
- [8] a) S. Volodarsky, I. Malahov, D. Bawari, M. Diab, N. Malik, B. Tumanskii, R. Dobrovetsky, *Chem. Sci.* **2022**, *13*, 5957–5963; b) M. Alcarazo, S. B. H. Karnbrock, C. Golz, R. A. Mata, *Angew. Chem. Int. Ed.* **2022**, *61*, e20220745.
- [9] D. Maiti, S. L. Buchwald, *J. Am. Chem. Soc.* **2009**, *131*, 17423–17429.
- [10] T. Thorwart, D. Hartmann, L. Greb, *Chem. Eur. J.* **2022**, *28*, e2022022.
- [11] All isolated compounds originating from **1c** (**2c**, **3c**) and reaction products of **3c** (**4**, **9**, **10**, **11**, **17**) contain ~9% of derivatives with a mono-hydrodefluorinated ligand backbone stemming from ligand synthesis. These derivatives were impossible to eliminate or separate at any stage. The outcome and the interpretation for this work remain unaffected.
- [12] M. Linnemannstons, J. Schwabedissen, B. Neumann, H. G. Stammler, R. J. F. Berger, N. W. Mitzel, *Chem. Eur. J.* **2020**, *26*, 2169–2173.
- [13] a) C. Riplinger, F. Neese, *J. Chem. Phys.* **2013**, *138*, 034106; b) C. Riplinger, B. Sandhoefer, A. Hansen, F. Neese, *J. Chem. Phys.* **2013**, *139*, 134101; c) F. Weigend, R. Ahlrichs, *Phys. Chem. Chem. Phys.* **2005**, *7*; d) A. Najibi, L. Goerigk, *J. Chem. Theory Comput.* **2018**, *14*, 5725–5738; e) F. Neese, *Wiley Interdiscip. Rev.: Comput. Mol. Sci.* **2012**, *2*, 73–78.
- [14] a) U. Mayer, V. Gutmann, W. Gerger, *Monatsh. Chem.* **1975**, *106*, 1235–1257; b) M. A. Beckett, G. C. Strickland, J. R. Holland, K. Sukumar Varma, *Polymer* **1996**, *37*, 4629–4631; c) P. Erdmann, L. Greb, *Angew. Chem. Int. Ed.* **2022**, *61*, e202114550.
- [15] a) S. Kozuch, D. Gruzman, J. M. L. Martin, *J. Phys. Chem. C* **2010**, *114*, 20801–20808; b) S. Grimme, A. Hansen, S. Ehlert, J.-M. Mewes, *J. Chem. Phys.* **2021**, *154*; c) A. V. Marenich, C. J. Cramer, D. G. Truhlar, *J. Phys. Chem. B* **2009**, *113*, 6378–6396; d) S. Grimme, J. Antony, S. Ehrlich, H. Krieg, *J. Chem. Phys.* **2010**, *132*, 154104.
- [16] G. A. Abakumov, A. I. Poddel'sky, E. V. Grunova, V. K. Cherkasov, G. K. Fukin, Y. A. Kurskii, L. G. Abakumova, *Angew. Chem. Int. Ed.* **2005**, *44*, 2767–2771; *Angew. Chem.* **2005**, *117*, 2827–2831.
- [17] While scXRD of the product remained unsuccessful so far, structural evidence for the phosphalkoxylation was obtained for products with related O,O-substituted phosphonium ions.
- [18] P. Löwe, M. Feldt, M. A. Wünsche, L. F. B. Wilm, F. Dielmann, *J. Am. Chem. Soc.* **2020**, *142*, 9818–9826.
- [19] F. Scholz, D. Himmel, F. W. Heinemann, P. v. R. Schleyer, K. Meyer, I. Krossing, *Science* **2013**, *341*, 62–64.

Manuscript received: September 28, 2022  
Accepted manuscript online: November 11, 2022  
Version of record online: December 16, 2022